

# Damage Detection in Cryogenic Composites for Space Applications Using Piezoelectric Wafer Active Sensors

Giola S. Bottai<sup>1</sup>, Patrick J. Pollock<sup>2</sup>, Thomas A. Behling<sup>3</sup>, and Victor Giurgiutiu<sup>4</sup>  
*University of South Carolina, Columbia, SC, 29208*

*and*

Scott M. Bland<sup>5</sup>, Shiv P. Joshi<sup>6</sup>  
*NextGen Aeronautics Inc, Torrance, CA, 90505*

Lamb waves have proven to be effective for damage detection by passively listening for emitted signals from crack growth or actively interrogating the structure. Acoustic emission sensors are used for monitoring a wide number of defects in materials such as dynamic strain, crack growth, leakage, corrosion, delamination, and fiber breakage in composite structures. The present paper will present an extensive experimental evaluation of the structural health monitoring (SHM) capability of the PWAS on composite structures of different geometries, environmental conditions, and stress conditions. Results from these experiments indicate that a PWAS based array is capable of detecting low velocity impact damage in composite materials. These experiments showed that abrupt changes in the DI occurred for sensor paths near the impact damage sites, which also indicates that localization of the damage is feasible using PWAS based arrays for SHM. The robustness of the PWAS arrays is demonstrated for damage detection at ambient, cryogenic, and cryogenic temperatures under uniaxial loading using both pulse-echo and pitch-catch methods. Based on these results, a PWAS based SHM array is shown to be a promising method for impact damage detection in composite materials, even in extreme conditions.

## Nomenclature

$d_{31}$	=	Piezoelectric constant
$E_1$	=	Axial modulus
$E_2$	=	Transverse modulus
$E/M$	=	Electromechanical impedance
$G_{12}, G_{23}$	=	Shear modulus
$g$	=	grams
$\nu_{12}, \nu_{23}$	=	Poisson's ratio
$P-C$	=	Pitch-Catch
$P-E$	=	Pulse-Echo

---

<sup>1</sup> Graduate Research Assistant, Department of Mechanical Engineering, University of South Carolina, 300 Main St. Columbia, SC 29208 USA. Tel: 803-777-0619 Fax: 803-777-0106; bottai@engr.sc.edu.

<sup>2</sup> Undergraduate Research Assistant, Department of Mechanical Engineering, University of South Carolina, 300 Main St. Columbia, SC 29208 USA. Tel: 803-777-0619 Fax: 803-777-0106; pollocpj@engr.sc.edu.

<sup>3</sup> Undergraduate Research Assistant, Department of Mechanical Engineering, University of South Carolina, 300 Main St. Columbia, SC 29208 USA. Tel: 803-777-0619 Fax: 803-777-0106; behlingt@engr.sc.edu.

<sup>4</sup> Professor, Department of Mechanical Engineering, University of South Carolina, 300 Main St. Columbia, SC 29208, USA. Tel: 803-777-8018; Fax: 803-777-0106; giurgiut@engr.sc.edu.

<sup>5</sup> Engineer, NextGen Aeronautics Inc. 2000 Kraft Drive Suite 2300, Blacksburg VA, 24060 USA; Tel: 540-443-9242; sbland@nextgenareo.com

<sup>6</sup> Chief Technology Officer, NextGen Aeronautics Inc. 2780 Skypark Drive, Suite 400, Torrance CA, 90505 USA; Tel: 310-626-8360; sjoshi@nextgenareo.com

Report Documentation Page				Form Approved OMB No. 0704-0188	
Public reporting burden for the collection of information is estimated to average 1 hour per response, including the time for reviewing instructions, searching existing data sources, gathering and maintaining the data needed, and completing and reviewing the collection of information. Send comments regarding this burden estimate or any other aspect of this collection of information, including suggestions for reducing this burden, to Washington Headquarters Services, Directorate for Information Operations and Reports, 1215 Jefferson Davis Highway, Suite 1204, Arlington VA 22202-4302. Respondents should be aware that notwithstanding any other provision of law, no person shall be subject to a penalty for failing to comply with a collection of information if it does not display a currently valid OMB control number.					
1. REPORT DATE <b>2008</b>		2. REPORT TYPE <b>N/A</b>		3. DATES COVERED <b>-</b>	
4. TITLE AND SUBTITLE <b>Damage Detection in Cryogenic Composites for Space Applications Using Piezoelectric Wafer Active Sensors</b>				5a. CONTRACT NUMBER	
				5b. GRANT NUMBER	
				5c. PROGRAM ELEMENT NUMBER	
6. AUTHOR(S)				5d. PROJECT NUMBER	
				5e. TASK NUMBER	
				5f. WORK UNIT NUMBER	
7. PERFORMING ORGANIZATION NAME(S) AND ADDRESS(ES) <b>Department of Mechanical Engineering, University of South Carolina, Columbia, SC 29208</b>				8. PERFORMING ORGANIZATION REPORT NUMBER	
9. SPONSORING/MONITORING AGENCY NAME(S) AND ADDRESS(ES)				10. SPONSOR/MONITOR'S ACRONYM(S)	
				11. SPONSOR/MONITOR'S REPORT NUMBER(S)	
12. DISTRIBUTION/AVAILABILITY STATEMENT <b>Approved for public release, distribution unlimited</b>					
13. SUPPLEMENTARY NOTES <b>The original document contains color images.</b>					
14. ABSTRACT					
15. SUBJECT TERMS					
16. SECURITY CLASSIFICATION OF:			17. LIMITATION OF ABSTRACT <b>UU</b>	18. NUMBER OF PAGES <b>15</b>	19a. NAME OF RESPONSIBLE PERSON
a. REPORT <b>unclassified</b>	b. ABSTRACT <b>unclassified</b>	c. THIS PAGE <b>unclassified</b>			

## I. Introduction

Structural health monitoring (SHM) is an emerging technology area with multiple applications in the evaluation of critical structures. The goal of current SHM research is to develop a monitoring system that is capable of detecting and identifying various damage modes during the service life of the structure with minimal human intervention. Numerous approaches have been utilized over the past three decades to perform structural health monitoring<sup>1-4</sup> and they can be broadly classified into two categories: passive methods and active methods. Passive methods, such as acoustic emission, have been heavily developed and are relatively mature methods, but suffer from the some significant drawbacks which have limited their utility. Active SHM methods are currently of great interest due to their greater versatility and the ability to interrogate a structure at any time. One of the most promising active SHM methods utilizes arrays of piezoelectric wafer active sensors (PWAS) bonded to a structure to both transmit and sense ultrasonic elastic waves for damage detection purposes<sup>5-7</sup>. When used to interrogate thin plate structures, these PWAS are effective Lamb wave transducers. The PWAS couple their in-plane motion with the Lamb wave particle motion on the material surface. The in-plane PWAS motion is excited by the applied oscillatory voltage through the  $d_{31}$  piezoelectric coupling. Optimum excitation and detection happens when the PWAS length is an odd multiple of the half wavelength of particular Lamb wave modes. The principle of wave generation through PWAS is fundamentally different from that of conventional ultrasonic transducers. Conventional ultrasonic transducers act through surface tapping, applying vibrational pressure to the object's surface. PWAS, on the other hand, act through surface pinching, and are strain coupled with the object surface. This allows PWAS to have a greater efficiency in transmitting and receiving ultrasonic surface and Lamb waves compared to conventional ultrasonic transducers.

Due to the increased use of composite materials in numerous types of structures, particularly in air and spacecraft structures, it is important that an active SHM system is capable of reliably detecting damage in these types of materials. One of the most troubling forms of damage in laminar composites is low velocity impact damage. This type of damage can leave no visual traces, but subsurface delaminations can significantly reduce the strength of the structure. The present work will investigate the use of PWAS to generate and sense ultrasonic Lamb waves to detect the presence of low velocity impact damage in composite panels.

### A. State of the Art

Previous research<sup>8-13</sup> has been focused on investigating the possibility of using embedded ultrasonic non-destructive evaluation and the opportunity for developing embedded structural health monitoring. Wave propagation methods were used for detection of cracks, corrosion and disbonds in stiffened metallic panels. Also, the ability to detect cracks under bolts and rivets was investigated. It was found that successful damage detection can be achieved using wave propagation methods as well as the electromechanical impedance method. A comparison of the damage detection methods for various damage types is given in Table 1.

**Table 1. Summary of PWAS damage detection methods.**

<b>Method</b> <b>Damage</b>	<b>Wave Propagation</b>			<b>Standing Wave</b>
	<b>Pitch-Catch</b>	<b>Pulse-echo</b>	<b>Phased-Array</b>	<b>EM Impedance</b>
Disbond	Fair	Excellent	--	Excellent
Cracks	--	--	Excellent	Fair
Corrosion	--	--	--	Excellent
Crack under bolt	Excellent	Fair	--	Fair
Delamination	Excellent	Excellent	--	Excellent

#### 1. Pitch-Catch Method

Pitch-catch method (Fig. 1a) can be used to detect structural changes that take place between a transmitter transducer and a receiver transducer. The detection is performed through the examination of the Lamb wave amplitude, phase, dispersion, and time of flight in comparison with a "pristine" situation. Typical applications include: (a) corrosion detection in metallic structures; (b) diffused damage in composites; (c) disbonds detection in adhesive joints; (d) delamination detection in layered composites, etc. The pitch-catch method can also be used to detect the presence of cracks from the wave signal diffracted by the crack.

## 2. Pulse-Echo Method

The use of Lamb wave pulse-echo methods with embedded PWAS follows the general principles of conventional Lamb wave non-destructive evaluation (NDE). A PWAS transducer attached to the structure acts as both transmitter and detector of Lamb waves traveling in the structure. The wave sent by the PWAS is partially reflected at the crack. The echo is captured at the same PWAS acting as receiver (Fig. 1b). For the method to be successful, it is important that a low-dispersion Lamb wave is used. The selection of such a wave is achieved through the Lamb-wave tuning methods<sup>5</sup>.

## 3. Electro-Mechanical Impedance Method

The impedance method is a damage detection technique complementary to the wave propagation techniques. The mechanical impedance method consists of exciting vibrations of bonded plates using a specialized transducer that simultaneously measures the applied normal force and the induced velocity. The principles of the EM impedance technique are illustrated in Fig. 1c). The electromechanical impedance method is applied by scanning a predetermined frequency range in the hundreds of kHz band and recording the complex impedance spectrum. By comparing the impedance spectra taken at various times during the service life of a structure, meaningful information can be extracted pertinent to structural degradation and the appearance of incipient damage. It must be noted that the frequency range must be high enough for the signal wavelength to be significantly smaller than the defect size.

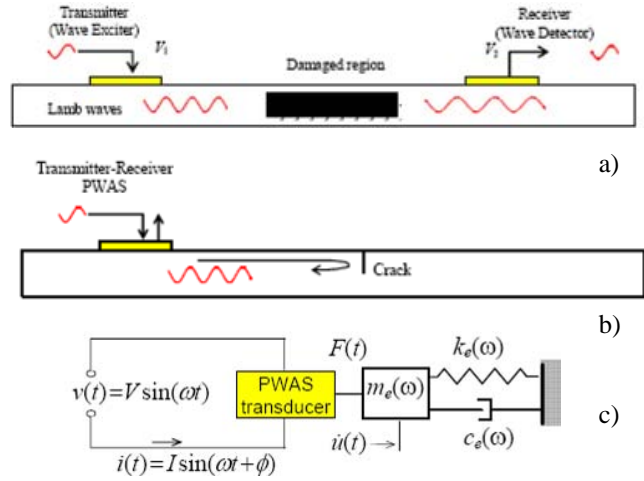


**Figure 1. Embedded ultrasonic damage detection: a) pitch-catch method; b) pulse-echo method; c) electromechanical impedance method.**

## B. Lamb Wave and PWAS Tuning on Plates

Lamb waves are a type of elastic wave that remain guided between two parallel free surfaces, such as the upper and lower surfaces of a plate or shell. Lamb wave theory is fully documented in a number of textbooks (Viktorov; Graff; Achenbach; Rose). The wave equation in the case of an isotropic media can be expressed through two potential functions and the longitudinal and shear wave velocity characteristic of the material of the media. The shear horizontal wave propagation in this case is decoupled from the longitudinal (or pressure waves P) and shear vertical (SV) wave propagations, and can be studied separately. For the case of a plate with free boundaries, the P and SV waves are coupled and their interaction is referred to as Lamb wave. Lamb waves modes can be symmetric and antisymmetric with respect to the through the thickness plane. The characteristic equation (Rayleigh-Lamb equation) of this type of waves is obtained by solving the wave equation and by applying stress free boundary conditions at the upper and lower surface. The phase velocity changes with the frequency and the thickness of the material. For each material, there exists a threshold value, dependent by the material of the plate, below which only S0 and A0 modes exist. In the case of composite materials it is not possible to find a close form solution of the dispersion curves, but there are different methods (transfer matrix, global matrix, and stiffness matrix) that can be used to solve the problem.

Currently, the most commonly used Lamb wave transducers are piezoelectric wedge transducers which can be setup to excite the particular modes needed for the structural interrogation. These wedge transducers are bulky, and are not appropriate for SHM in aerospace applications. PWAS transducers are much smaller than wedge transducers, and can be used for SHM applications, but they excite all of the Lamb wave modes existing at the given frequency-thickness product. The simultaneous presence of two or more modes increases the difficulty of the damage detection process. The ability to excite a single wave mode is therefore important to allow for effective damage detection. By tuning the PWAS as shown in Refs. 14 and 15, a single wave mode can be predominantly excited using a PWAS. These references report the theoretical results for the infinite actuator strip and for the circular actuator respectively. Tuning between PWAS and an anisotropic host structure has also been experimental demonstrated<sup>16</sup>. Pitch-catch experiments were performed in which one PWAS served as Lamb wave transmitter and another PWAS served as receiver. Experiments were performed with round PWAS diameter 7 mm, 0.2 mm thick (American Piezo Ceramics APC-850) bonded to a quasi-isotropic plate. Three waves were detected: S0, A0, and

SH0. The experiments clearly showed the presence of tuning between the PWAS and the composite material. The tuning frequency was the same in every direction due to the quasi-isotropic nature of the material. The A0 amplitude disappeared or became very low at the S0 maximum. It was not possible to actuate the S0 mode alone due to the presence of the SH mode.

## II. Description of the Experiments

The basic element used for damage detection in these experiments was a round 7 mm diameter, 0.2 mm thick PWAS. The piezoelectric material was found to be able to maintain actuation abilities in the cryogenic environments. The signal generated by the PWAS at cryogenic temperature (CT) had amplitudes smaller than the signal generated at room temperatures (RT). After the PWAS returned to RT after being exposed to CT, the signal amplitudes increased, but were still lower than the original signal before exposure to CT. Standing wave generation via electro-mechanical impedance and elastic wave transmission and reception abilities were performed using PZT PWAS bonded on unidirectional composite beams. Figure 2 shows impedance signatures taken from PZT PWAS after every submersion up to 10 submersions in liquid nitrogen. It can be seen that the material retains its peaks and their relative frequency location shows a wave packet propagated using PZT PWAS before, during and after submersion in liquid nitrogen. It should be noted that the signal propagated in the nitrogen has smaller peak to peak amplitude, but at the same time has proportionately smaller background noise. The amplitude at RT after submersion in liquid nitrogen did not return to original amplitudes. These experiments were conducted with the transducers in direct contact with the liquid nitrogen. In real application the transducer will be not necessarily be in contact with the liquid nitrogen.

The adhesive layer between the PWAS and the structure is a critical aspect. Incorrect thickness, porosity, poor chemical preparation, etc. leads to poor transmission of shear energy. The adhesive selected was Vishay M-Bond AE-15 (2-component). Su/Pb solder was used for standard RT applications, but at CT, Pb becomes brittle. Indium was used in CT applications because of the materials ability to retain mechanical properties even at CT.

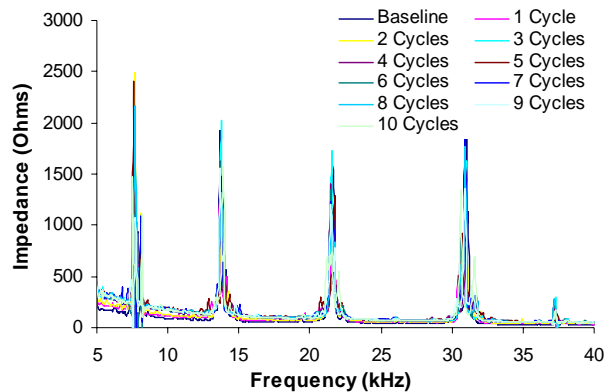


**Figure 2. Indication of survivability through resumption of resonant properties after submersion in liquid nitrogen (PZT PWAS, AE-15, room temperature).**

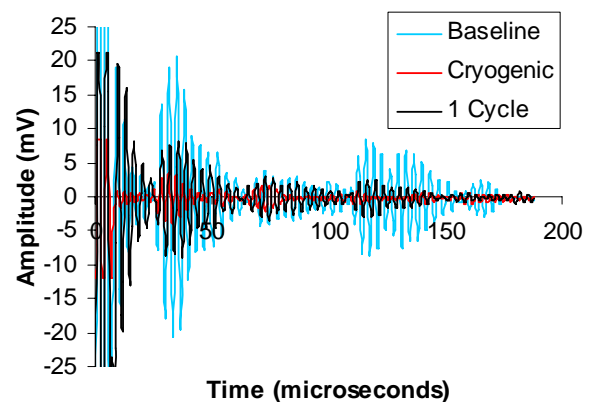


**Figure 3. Wave propagation in composite for various thermal environments. Comparison of a wave packet before, during, and after submersion in liquid nitrogen.**

In order to test the performance of the PWAS on various types of composite materials and structures commonly found in space applications four different test specimens were utilized. The first type of specimen was a composite strip made of unidirectional fibers. The specimen was 400 x 51 mm (16"x2") and 1 mm thick. The fibers direction was parallel to the longest direction of the specimen. A schematic of this specimen is shown in Fig. 4. We used the unidirectional strips to test damage detection of through holes at room temperature.

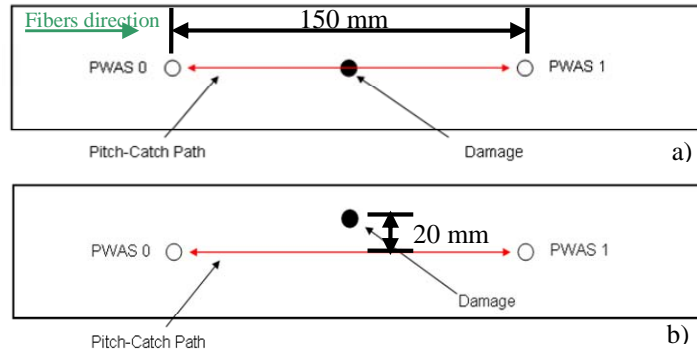


**Figure 4. Unidirectional composite strips with PWAS installed. a.) hole in the pitch-catch path; b.) hole skewed from the pitch-catch path.**

The second type of specimen was a quasi-isotropic composite plate  $[(0/45/90/-45)_2]_s$ , of A534/AF252 Uni Tape with 2.25 mm thickness and  $1.236 \times 1.236$  m size (4'x4'). The composite panel specimen was used to investigate the PWAS damage detection performance at room temperatures both for through-hole detection and impact damage detection. A schematic of the test specimen and experimental setup used during the experiments with the specimen are shown in Fig. 5.

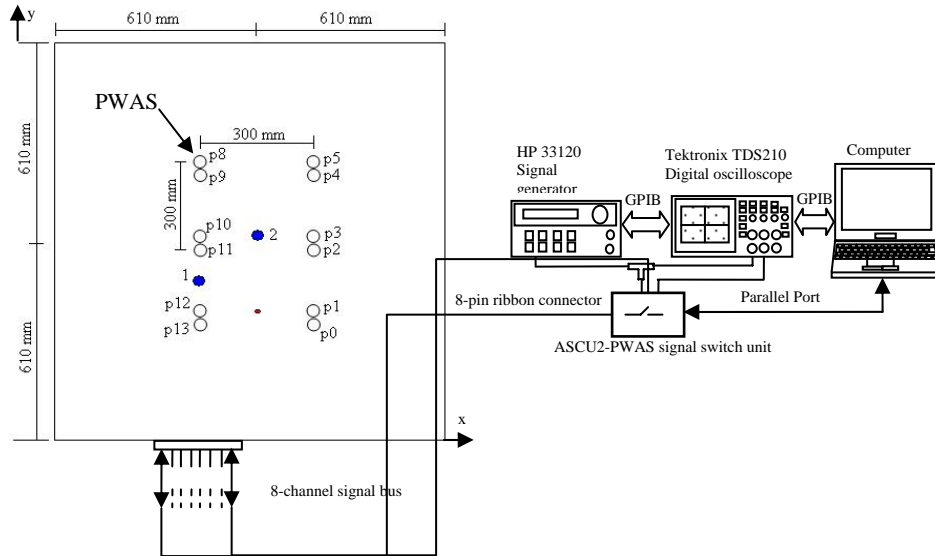


**Figure 5. Experimental setup for quasi-isotropic plate experiments. Red dots on plate: holes; blue dots on plate: impact.**

The third type of specimen utilized during the experimental characterization of the PWAS was a composite lap joint. The specimen had the same material and lay-up as the X-34 fuel tank. The geometry of the specimen is shown in Fig. 6. The specimen was built with 16 seeded defects inside (Teflon patches), 8 on two rows distant respectively 76.2 mm (3") and 152.4 mm (6") from the longitudinal edge. The 8 patches in each row are approximately equidistant. We performed the following tests on this specimen: damage detection at room temperature with PWAS pair 1; damage detection at

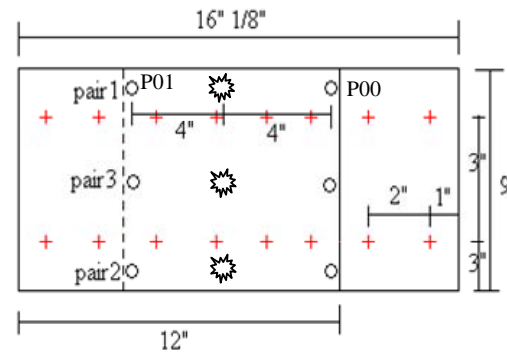


**Figure 6. a) Lap joint; Teflon patches location (red crosses) and PWAS location (circles).**

cryogenic temperature with PWAS pair 2; damage detection at cryogenic temperature under uni-axial load with PWAS pair 3.

The fourth type of specimen utilized during the experimental testing was a composite tank interface. This specimen also had the same material and lay-up as the X-34 fuel tanks. The composite tank interface specimen had plate of dimension 304.8 x 228.6 mm (12"x9"). The specimen was fabricated with 16 patches of different sizes located between various plies. Two experiments were performed on the specimen: patch detection at room temperature; patch detection at cryogenic temperature.

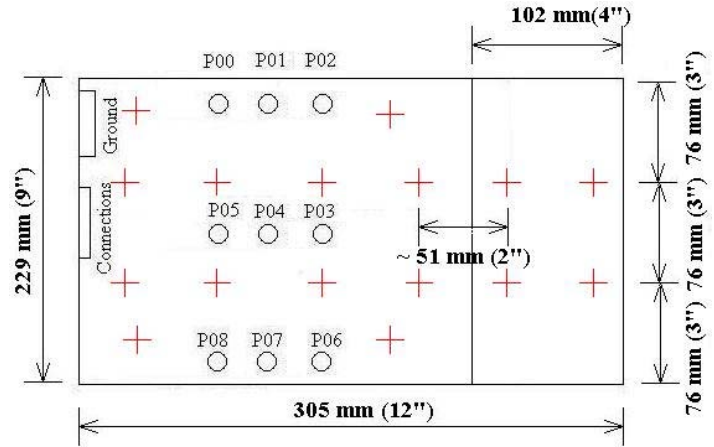


**Figure 7. Schematic of composite tank interface specimen and location of Teflon inserts (crosses).**

Table 2 shows the specimens used, the type of damage, the environmental condition, and the method used in the experiments. The data collected in each experiment were analyzed using a damage index (DI). The DI was used to assess the severity of the damage in each test run. The damage index is a scalar quantity that results from the comparative processing of the signal under consideration. The damage metric should reveal the difference between readings (impedance spectrum or wave packets) due to the presence of damage. Ideally, the damage index would be a metric, which captures only the spectral features that are directly modified by the damage presence, while neglecting the variations due to normal operation conditions (i.e., statistical difference within a population of specimens, and expected changes in temperature, pressure, ambient vibrations, etc.). To date, several damage metrics have been used to compare impedance spectra or wave packages and assess the presence of damage. Among them, the most popular are the root mean square deviation (RMSD), the power, the mean absolute percentage deviation (MAPD), and the correlation coefficient deviation (CCD). In our experiments we have used the RMSD DI shown in Equation 1.

$$RMSD = \sqrt{\frac{\sum_n \{ \text{Re}(S_i) - \text{Re}(S_i^0) \}^2}{\sum_n \{ \text{Re}(S_i^0) \}^2}} \quad (1)$$

RMSD yields a scalar number, which represents the relationship between the compared readings. The advantage of using this method is that the data do not need any preprocessing, i.e., the data obtained from the measurement equipment can be directly used to calculate the damage index.

**Table 2. Summary of experiments discussed in this paper.**

Specimen	Damage	Environment	Loading	Methods
Unidirectional strips	Hole	RT	Free	P-C
Composite panel	Hole Impact damage	RT	Free	P-C, P-E
Lap-joint	Impact damage	RT CT	Free Free Uniaxial load	P-C
Tank interface	Delamination	RT CT	Free	P-C

### III. Damage Detection Experiments on Test Specimens

#### A. Unidirectional Composite Strips

The initial testing of the PWAS based damage detection began with unidirectional strips shown in Fig. 4. In both strips we installed two round PWAS 150 mm apart and we used the pitch-catch method to detect the damage. In the first experiment we determined the smallest through-hole diameter that was detectable by the PWAS when the through-hole was centered with the PWAS. In the second experiment, we determined the smallest detectible hole diameter when the hole was offset 20 mm with respect to the pitch-catch path.

The first readings were taken when the strips were undamaged (baselines). Then, we drilled a 0.8 mm hole on both specimens, enlarged them in 11 steps until they reached 6.4 mm in diameter. Table 3 reports the dimension of the holes for each step and reading.

**Table 3. Hole sizes for corresponding readings in the unidirectional composite strip experiments.**

Step #	Readings	Hole size (mm)	Step #	Readings	Hole size (mm)
0	00 – 04	--	6	31 – 35	3.2
1	05 – 09	0.8	7	36 – 40	3.6
2	10 – 14	1.5	8	41 – 45	4.0
3	15 – 19	1.6	9	46 – 50	4.8
4	20 – 25	2.0	10	51 – 55	5.5
5	26 – 30	2.4	11	56 – 60	6.4

The excitation signals for the experiments on the unidirectional composite strips was a 3 count tone burst at 480 kHz, which resulted in the strongest S0 wave packet. The resulting signals were then analyzed using the RMSD DI and the results are shown in Fig. 8 for both the centered and off-center hole cases. Each dot in the graph represents a reading (there are 5 readings for each step to indicate reproducibility). The first 5 readings are the baseline; the strip without damage. As soon as the holes were drilled on the plate the DI value changed. The DI value changed rapidly as the damage size went from 2 mm to 2.4 mm.

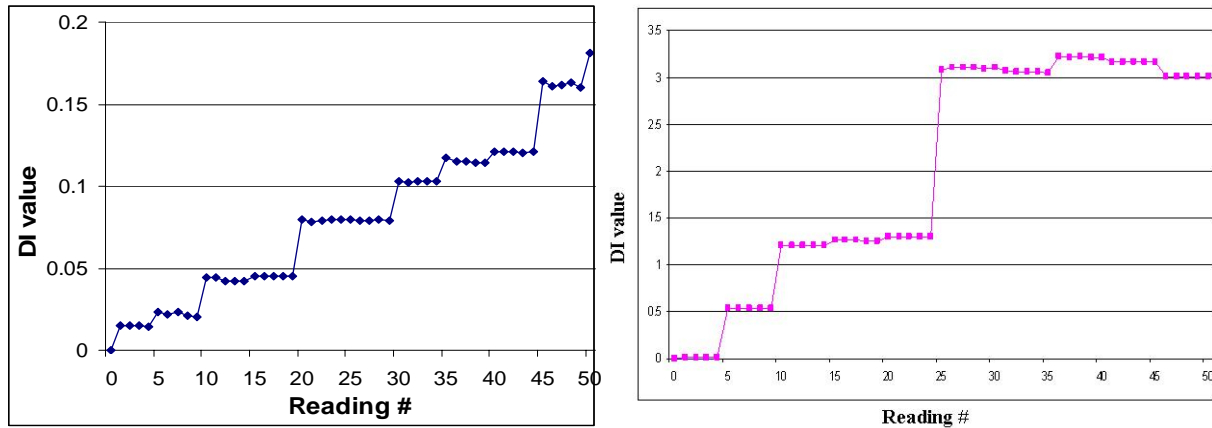


**Figure 8. DI analysis of the damaged unidirectional composite strip. a.) Hole in the pitch-catch path; b.) Hole skewed from the pitch-catch path.**

Fig. 8a shows that the DI increases monotonically with the increasing hole size which will allow for easy interpretation of the DI in relation to the damage size. Figure 8b also shows a monotonically increasing DI value relative to the hole size initially, but the DI value plateaus for hole sizes greater than 3.2 mm. This indicates that off-axis damage in unidirectional composites may be more difficult to detect and identify compared to centered damage.



## B. Quasi-Isotropic Composite Laminate

The next test specimen that was examined was a quasi-isotropic composite plate discussed previously. Two different forms of damage, through-holes and impact damage, were investigated for this plate at room temperature conditions. Twelve PWAS were installed in an array on the quasi-isotropic composite plate as shown in Fig. 5 and the distance between the 6 PWAS pairs was 30 mm. In this case, the data was collected automatically through ASCU2 system with an input voltage of the signal from the function generator of 11 V (Fig. 5) because this is the maximum input voltage that is possible to send through ASCU2. The excitation signal used during the interrogations was a 3 count tone burst at 54 kHz, 225 kHz, and 255 kHz. These frequencies were selected through Lamb wave tuning experiments to maximize the A0, and S0 wave modes. At 54 kHz it possible to obtain the maximum pseudo A0 mode; at 255 kHz we obtain the maximum pseudo S0 mode; at 225 kHz we have the maximum pseudo S0 mode with the minimum amplitude of the other modes.

### 1. Detection of Through-Holes

In the through-hole detection case, data was collected from PWAS 0, 1, 5, 8, 12, and 13. Each PWAS was in turn a transmitter and a receiver. Readings were taken with the plate in an undamaged state and the plate in a damaged state. Four baseline readings were taken in the undamaged configuration. A hole was drilled between PWAS 1 and 12. The location of the hole was halfway between these two PWAS. The diameter of the hole was increased in 14 steps. At each step several readings were recorded. Table 4 reports the step number, the number of readings recorded at each step, and the hole dimension at each step. Each reading was compared to the baseline reading 00 through DI analysis. The DI value was computed through RMSD DI shown in Equation 1.

**Table 4. Hole diameters corresponding to the quasi-isotropic plate damage detection experiment.**

Step	Reading #	Hole size in mil [mm]	Step	Reading #	Hole size in mil [mm]
1	00 – 03	0	2	04 – 07	032 [0.8]
3	08 – 11	059 [1.5]	4	12 – 15	063 [1.6]
5	16 – 19	078 [2.9]	6	20 – 23	109 [2.8]
7	24 – 28	125 [3.2]	8	29 – 32	141 [3.5]
9	33 – 36	156 [4.0]	10	37 – 40	172 [4.4]
11	41 – 44	188 [4.8]	12	45 – 48	203 [5.2]
13	49 – 52	219 [5.5]	14	53 – 56	234 [6.0]

For the pitch-catch analysis we took in consideration only the data coming from the following PWAS configuration:

1. PWAS 0 transmitter, PWAS 13 receiver;
2. PWAS 1 transmitter, PWAS 12 receiver;
3. PWAS 5 transmitter, PWAS 8 receiver.

The data from this experiment allowed for the determination of the minimum hole diameter that the two PWAS pairs (00 – 13, 01 – 12) were able to detect. We use also PWAS pair 05 – 08 to see whether there was any difference with the PWAS pairs close to the damage. At an excitation frequency of 54 kHz, only the A0 mode is present. The wave velocity of the A0 mode in this material is 1580 m/sec; the wavelength is 29.3 mm. Fig. 9 shows the box plot of the DI values for the three different PWAS pairs. As the hole diameter increases, the DI values for the two PWAS pairs

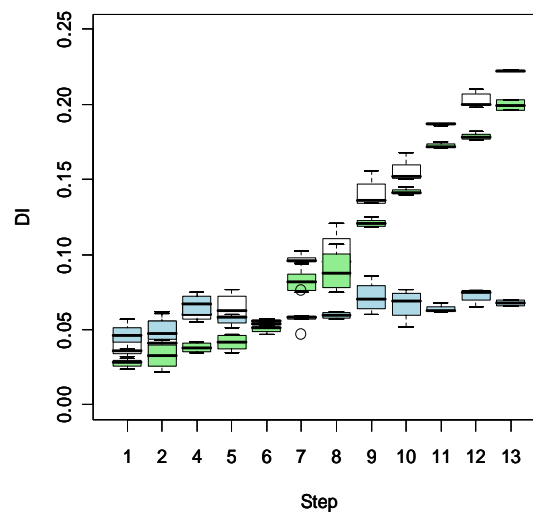


**Figure 9. DI values at different hole sizes and PWAS pairs using an excitation frequency of 54 kHz.**

close to the hole increase while the DIs for the PWAS pair 05 – 08 remain almost the same. We analyzed the data with statistical software (SAS) and we observed that with a significance of 99%, PWAS pair 1 – 12 can detect the presence of the hole when its diameter is 2.8 mm; PWAS pair 0 – 13 could detect the presence of the hole when its diameter is 3.18 mm. There was no significant difference between the DI values of PWAS pair 5 – 8.

At an excitation frequency of 225 kHz only the S0 mode is present in the quasi-isotropic plate. The wave velocity is about 6000 m/sec, the wavelength is 26.6 mm. Fig. 10 shows the box plot of the DI values for the three different PWAS pairs. As the hole diameter increases, the DI values for the two PWAS pairs close to the hole increases while the DI for the PWAS pair 05 – 08 remain almost the same. PWAS pair 0 – 13 and 1 – 12 could detect the presence of the hole when its diameter is 2.8 mm with a significance of 99%. There was no significant difference between the DI values of PWAS pair 5 – 8.

At an excitation frequency of 255 kHz, the S0 mode has maximum amplitude. The wave velocity is again about 6000 m/sec, the wavelength is 23.5 mm. Fig. 11 shows the box plot of the DI values for the two different PWAS pairs. As the hole diameter increases, the DI values for the two PWAS pairs close to the hole increases while the DI for the PWAS pair 05 – 08 remain almost the same. With a significance of 99%, PWAS pair 0 – 13 and PWAS pair 1 – 12 (not shown in the graph) could detect the presence of the hole when its diameter was 3.18 mm. There was no significant difference between the DI values of PWAS pair 5 – 8.

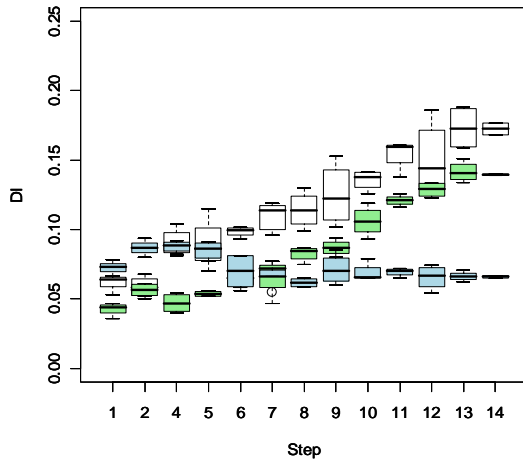


**Figure 10. DI values at different Step values and PWAS pair. Frequency 225 kHz**

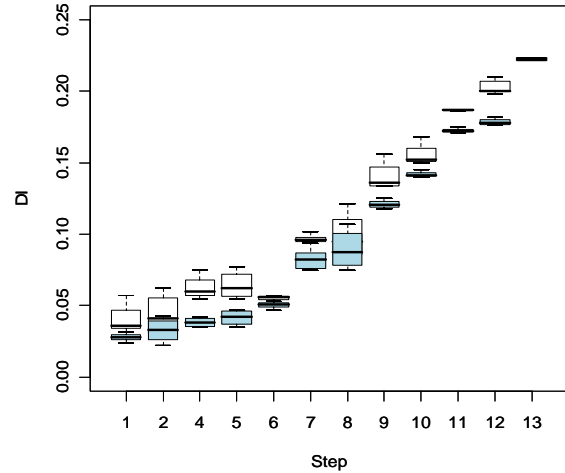


**Figure 11. DI values at different Step values and PWAS pair. Frequency 255 kHz.**

Pulse – echo analysis was performed for PWAS 0 – 1. PWAS 0 was used as transmitter while PWAS 1 was the receiver. Fig. 12 shows the DI box plot at different step values for an excitation frequency of 54 kHz. Analyzing the data with Tukey multiple comparison and we find that there was significant difference between step 1 (baseline) and step 7. We could detect the hole when its diameter was 3.2 mm with 99% confidence.

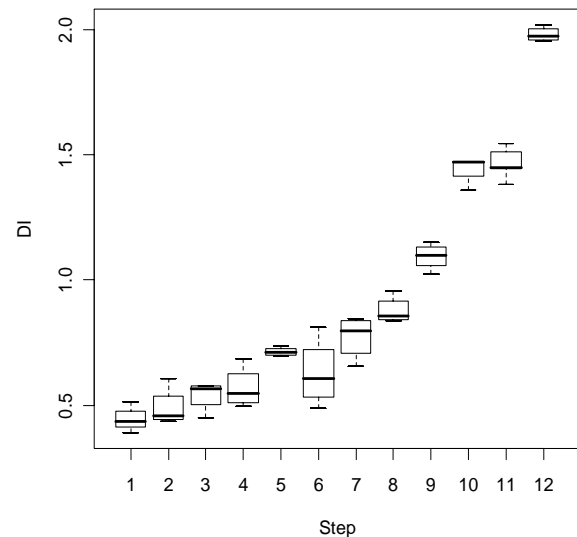


**Figure 12. DI values at different Step values, Frequency 54 kHz. Pulse – echo.**

## 2. Detection of Impact Damage

The second form of damage that was studied on the quasi-isotropic composite plate was impact damage. The impact damage was applied to the plate using the impactor shown in Fig. 13. The impactor had a hemispherical tip of 12.7 mm in diameter (0.5") and its weight was 391 g (13.79 oz). The impactor weight could be increased by adding barrels (Fig. 13b) to the base configuration of Fig. 13a. Each barrel weighted 500 g. (1 lb 1.63 oz); a total of 3 barrels could be assembled on the impactor.

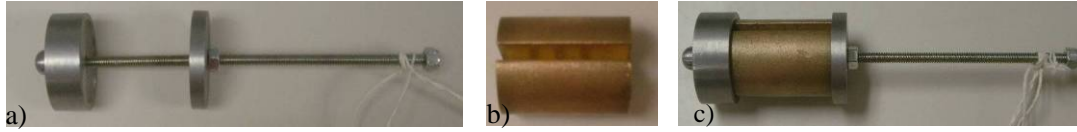


**Figure 13. a) Base impactor with hemispherical tip; b) barrel; c) impactor assembled.**

Two impact damages sites were produced on the plate with two different impactor configurations (respectively two barrels and one barrel). The impactor used for damage site A had a total weight of 1391 g (3 lb 1.1 oz). Two different impact damage states were created at this site by dropping the impactor from different heights. The first impact damage state had an impact energy level of 6 ft-lb and hit the plate at about 3.5 m/sec (11 ft/sec); the second impact damage state had an impact energy level of 12 ft-lb and hit the plate at about 5 m/sec (16 ft/sec).

**Table 5. Summary of impact test parameters on quasi-isotropic plate specimen.**

Damage Site	Readings	Energy m-kg (ft-lb)	Velocity m/sec (ft/sec)	Step
A	00 – 10			1
	11 – 20	0.83 (6)	3.5 (11)	2
	21 – 30	1.66 (12)	5 (16)	3
B	00 – 10			1
	11 – 20	0.83 (6)	4 (14)	2
	21 – 30	1.66 (12)	6 (20)	3

The impactor used for damage site B had a total weight of 891 g (1 lb 15.5 oz)). The first impact damage state had an impact energy level of 6 ft-lb and hit the plate at about 4 m/sec (14 ft/sec); the second impact damage state had an impact energy level of 12 ft-lb and hit the plate at about 6 m/sec (20 ft/sec). Table 5 shows the energy and velocity levels for the damage states at both damage sites. For both damage site A and damage site B, we recorded 11 baseline readings and 10 readings for each energy level. The readings were again collected through the ASCU2 system. The input voltage of the signal was limited to 11 V.

The first impact site (Damage A) was produced between PWAS 12 and PWAS 11 (see Fig. 5 for reference). No visual damage was produced at 6 ft-lb energy level. After the second impact at energy level of 12 ft-lb, damage could be seen on the opposite surface of the plate. We took the readings for PWAS pairs 11 – 12 and 09 – 10. Each PWAS of each pair was used once as a transmitter and once as a receiver. The second damage site (Damage B) was produced between PWAS 2 and PWAS 11 (see Fig. 5 for reference). We collected readings from PWAS pairs 2 – 11, 3 – 10, and 05 - 08. No visible damage was produced after the two impacts. However the presence of damage in the plate structure was registered through standard ultrasonic methods.

Figure 14 shows the DI values for damage site A for an excitation frequency of 54 kHz. There is little difference between the DI values of the PWAS pair (09 – 10) far from the impact damage. The PWAS pair with the damage in between shows a significant DI change after the second impact (energy level 12 ft-lb) indicating that it is possible to detect the damage after the second impact. The DI values for damage site B at 54 kHz were qualitatively the same as for damage site A. Figure 15 shows the DI values for the three different steps for damage site A. The PWAS pair that is far from the impact damage does not show much difference between the DI values of the three steps. The PWAS pair with the damage in between shows a DI change after the second impact (energy level 12 ft-lb), however, the change is not significant as in the case of frequency 54 kHz. The pseudo S0 mode is less sensitive to this kind of damage in the composite panel. Again, similar results were obtained for damage site B.

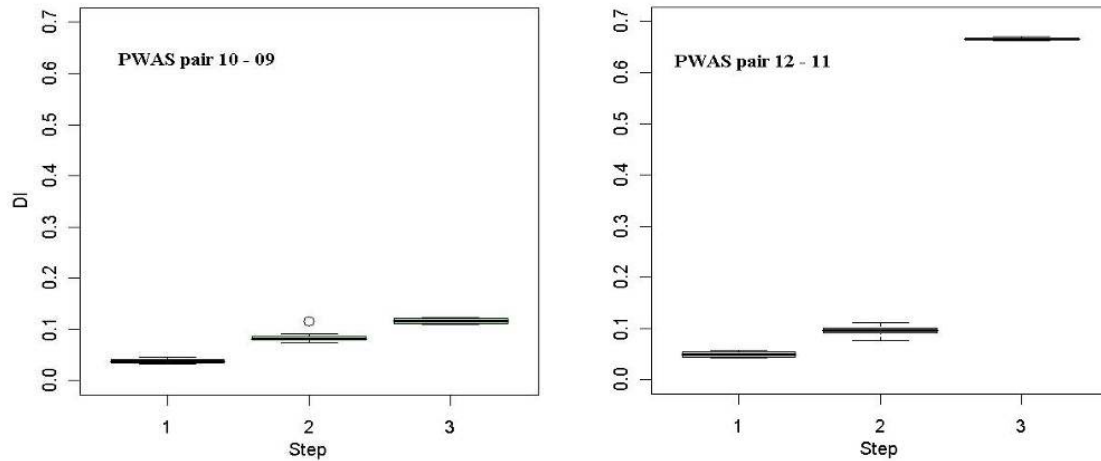


**Figure 14. DI values as a function of the damage level for two PWAS pairs at damage site A with an excitation frequency of 54 kHz.**

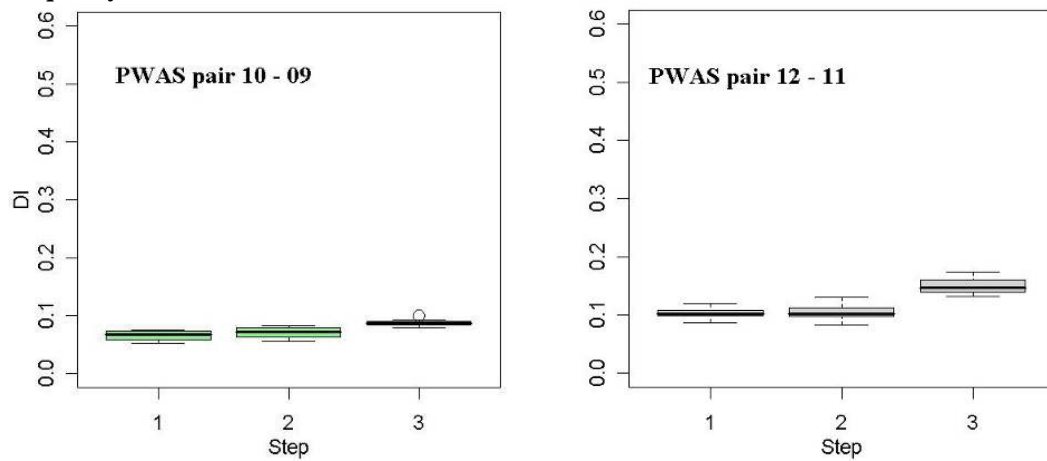


**Figure 15. DI values as a function of the damage level for two PWAS pairs at damage site A with an excitation frequency of 225 kHz.**

Pulse – echo analysis was performed for PWAS 11 – 10 on damage site A. PWAS 11 was used as transmitter while PWAS 10 was the receiver. Figure 16 shows the DI box plot at different step values and excitation frequencies for damage site A. Analyzing the data we find that there is a statistically significant difference between step 1 (baseline) and other two steps for the case of 54 kHz, while there is significant difference between Step 1 and Step3 (impact at 12 ft-lb) for the case of 225 kHz. As in the pitch-catch method, the S0 mode was less sensitive to impact damage.

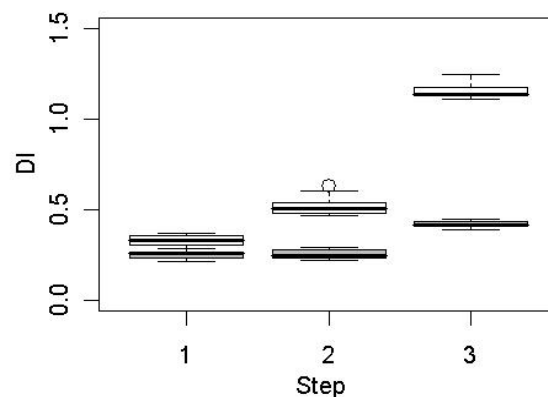


**Figure 16. DI values at different step values for damage site A. White box: excitation frequency of 54 kHz; Gray box: excitation frequency of 225 kHz.**

### C. Composite Lap-Joint

Damage detection experiments were also performed for a composite lap-joint specimen which had impact damage. The impactor configuration used in this case was the same as that used for damage site A on the composite plate (see Table 5). A total of 11 readings were taken in the undamaged baseline configuration, 10 readings were taken after the impact with energy level 6 ft-lb, and 10 readings were recorded after the impact at 12 ft-lb. The first reading of the baseline was used as the reference reading for the DI analysis. The test was divided in three steps (for each step we collected 10 readings).

The location of the PWAS and the impact sites on the lap-joint are shown in Fig. 6. Two columns of PWAS were installed on one side of the lapjoint; each column of PWAS was bonded close to one of the edges of the joint. The distance between the columns was 203.2 mm (8"). PWAS 00 represents the PWAS closest to the joint location. Each impact damage was located between PWAS pairs. The input voltage of the signal for these experiments was increased to 18 V to obtain a better signal to noise ratio. We used the Lamb wave tuning method to select the frequencies at which there was only the presence of one mode. We found that such conditions existed at 54 kHz and 318 kHz. The wave speed at 54 kHz was 1175 m/sec, the wavelength 21.8 mm. The wave speed at 318 kHz was 3065 m/sec, the wavelength 10 mm. Figure 17 shows the box – plots of the DI values for two different frequencies. Both low and high frequencies were able to detect impacts at 6 ft-lb and 12 ft-lb with a significance level of 99%.

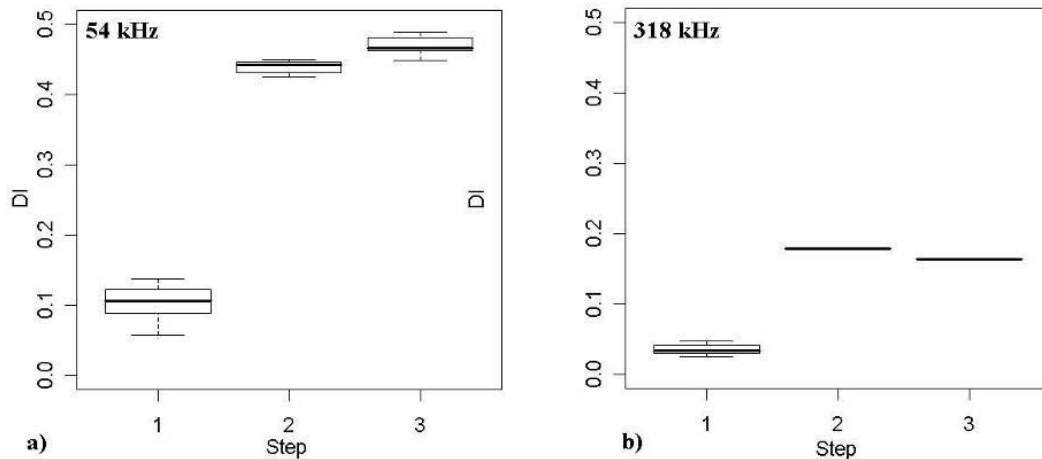


**Figure 17. DI values for different damage level (PWAS pair 00 – 02) at RT on the composite lap-joint specimen. a) excitation frequency of 54 kHz; b) excitation frequency of 318 kHz.**

The absolute difference at low frequency between step 1 and step 2 is much higher than the same difference at high frequency. This indicates that similar to the quasi-isotropic plate case, lower frequencies are more sensitive to impact damage at room temperature than the high frequency excitations. Since impact damage is a complicated form of damage involving multiple damage modes in the composite material, the DI values are sensitive to the pitch-catch paths used.

Similar tests were performed using the PWAS system for damage detection on the lap-joint at cryogenic temperatures. Two frequencies were selected through tuning: 60 kHz and 318 kHz. The wave speed at 60 kHz was 1410 m/sec, with a wavelength of 23 mm. The wave speed at 318 kHz was 3065 m/sec, with a wavelength of 10 mm. All the data collected in this case was at temperatures below -150° C. Figure 18 shows the box-plots of the DI values for the two different frequencies. Both low and high frequencies were able to detect the impacts produced at different energy levels (6 ft-lb and 12 ft-lb) with a significance level of 99 %.

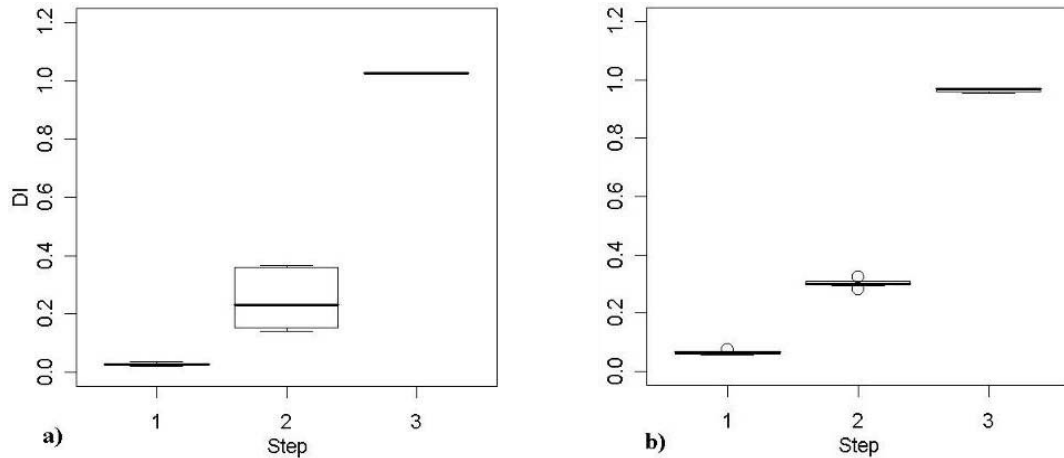


**Figure 18. DI values for different damage level (PWAS pair 00 – 02) at CT on the composite lap-joint specimen. a) excitation frequency of 54 kHz; b) excitation frequency of 318 kHz.**

As shown in Fig. 17 and Fig. 18 impact damage was detectable by the PWAS based array. Both high and low frequency excitations were sensitive to the impact damage; however, excitation at 54 kHz showed higher sensitivity in the RT case compared to the 318 kHz excitation.

#### **D. Composite Tank Interface Specimen**

Nine PWAS were installed composite tank specimen (Fig. 7). Readings taken with PWAS pair P01 – P04 and P07 – P04 were used as a baseline for the material because there were no patches in the wave path between these pairs. The experiments were performed to detect the presence of Teflon patches which were incorporated during manufacture of the specimen to simulate delaminations. Two experiments were performed on the specimen: Patch detection at room temperature; Patch detection at cryogenic temperature.

Based on the sample configuration, the following notation will be used:

1. Step 1 denotes the 4 DI values of the PWAS pair with no patch in between;
2. Step2 denotes the 5 DI values of the PWAS pair with patch in between and closer to the free edge of the plate (PWAS P00, P05, and P08);
3. Step 3 denotes the 5 DI values of the remaining pairs (patch location deeper in the thickness).

The composite tank interface specimen was scanned at two different frequencies: 60 kHz and 318 kHz. The speed of the wave at 60 kHz was about 2680 m/sec and the wavelength of the wave about 45 mm. At high frequency (318 kHz), it was not possible to determine the velocity. The experiments were again performed with an input voltage of 18 V to improve the signal to noise ratio. Figure 19 shows the DI values for the composite tank specimen at room temperature. Step 2 refers to the data recorded with PWAS pair P05– P00. From the analysis of the DI values we see that the low frequency is more sensitive to the patch depth, especially when the patches are large. The high frequency was more sensitive to the patch presence, but it is not affected by their depth or dimension.

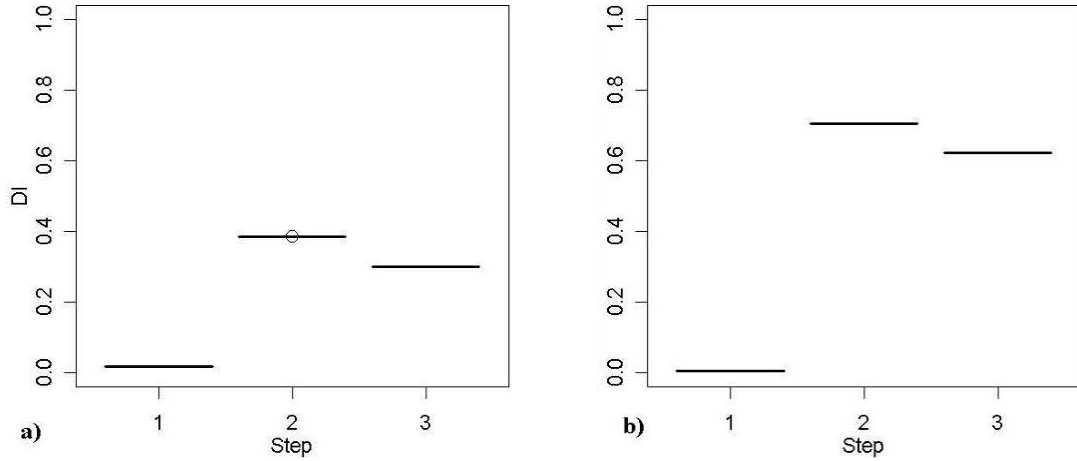


**Figure 19. Composite tank interface specimen, room temperature. a) excitation frequency of 54 kHz; b) excitation frequency of 318 kHz.**

A similar experiment was conducted at cryogenic temperatures. Readings were taken with temperatures below  $-150^{\circ}\text{C}$ . We used a different frequency for the low frequency case (75 kHz) because the cryogenic temperature caused a shift in the frequency of the maximum amplitude of the A0 mode. Figure 20 shows how DI index changed with the different steps. We found that there was significant difference between the steps; the PWAS were able to detect the presence of the patches. From the DI values we determined that both frequencies could detect the presence of the patches; however at 318 kHz there was greater sensitivity. The depth or the dimension of the patches did not affect the DI values.

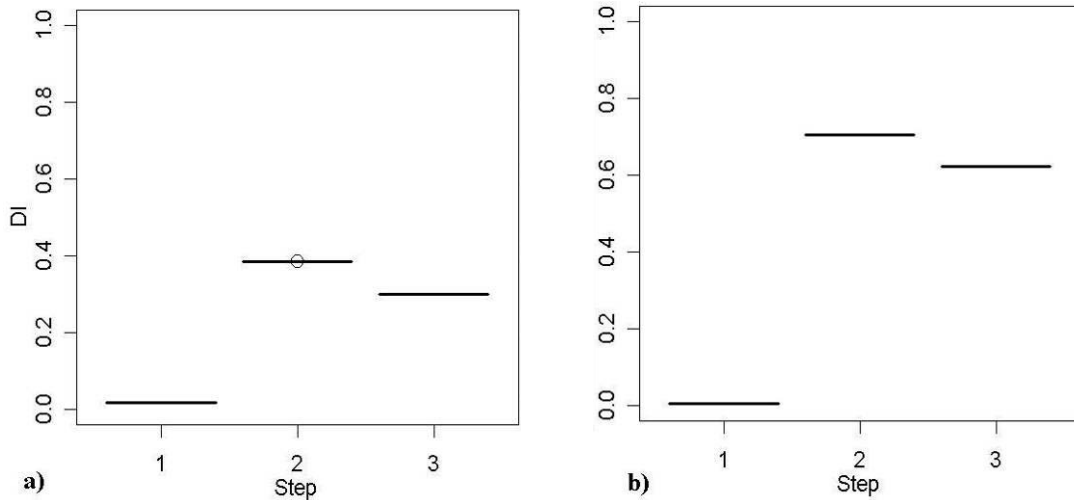


**Figure 20. Composite tank interface specimen, cryogenic temperature. a) excitation frequency of 75 kHz; b) excitation frequency of 318 kHz.**

#### IV. Conclusions

Based on the damage detection results presented here, it is shown that PWAS based arrays are effective for detecting multiple types of damage (through-holes, impact damage, and delaminations) in complex composite materials used in spacecraft applications. In particular, results were shown for damage detection of through-holes in unidirectional composite strips at room temperature, detection of through-holes and impact damage in a quasi-isotropic plate at room temperature, detection of impact damage on a composite lap-joint specimen at room and cryogenic temperatures, and detection of simulated delaminations in a composite tank interface at room and cryogenic temperatures. These results indicate that a PWAS based array would be effective and reliable for structural health monitoring on composite space vehicles.

## Acknowledgements

Research on this project was supported by the National Aeronautics and Space Administration, Langley Research Center, under contract NNL05AA44C. Such support does not constitute an endorsement by NASA of the views and opinions expressed in this article.

## References

- <sup>1</sup>Doebling, S. W., Farrar, C. R., Prime, M. B., and Shevitz, D. W., "Damage Identification and Health Monitoring of Structural and Mechanical Systems From Changes in Their Vibration Characteristics: A Literature Review," Los Alamos National Laboratory Report LA-13070-MS, May 1996.
- <sup>2</sup>Sohn, H., Farrar, C.R., Hemez, F. M., Shunk, D. D., Stinemates, S. W., Nadler, B. R., and Czarnecki, J. J., "A Review of Structural Health Monitoring Literature form 1996-2001," Los Alamos National Laboratory report LA-13976-MS, 2004.
- <sup>3</sup>Farrar, C.R., Sohn, H., Hemez, F.M., Anderson, M.C., Bement, M.T., Cornwell, P.J., Doebling, S.W., Schultze, J.F., Lieven, N., Robertson, A.N., "Damage Prognosis: Current Status and Future Needs," Los Alamos National Laboratory Report, LA-14051-MS, 2004
- <sup>4</sup>Rose, J.L., Soley, L., "Ultrasonic guided waves for the detection of anomalies in aircraft components", *Materials Evaluation*, Vol. 50, No. 9, pg. 1080-1086, 2000.
- <sup>5</sup>Giurgiutiu, V., "Lamb Wave Generation with Piezoelectric Wafer Active Sensors for Structural Health Monitoring", *SPIE's 10th Annual International Symposium on Smart Structures and Materials and 8th Annual International Symposium on NDE for Health Monitoring and Diagnostics*, 2-6 March 2003, San Diego, CA, paper # 5056-17
- <sup>6</sup>Giurgiutiu, V., Zagrai, A., Bao, J. J., Redmond, J. M., Roach, D., and Rackow, K. "Active Sensors for Health Monitoring of Aging Aerospace Structures," *International Journal of COMADEM*, Vol. 6, No. 1, pg 3–21, 2003.
- <sup>7</sup>Giurgiutiu, V., Zagrai, A., Bao, J., "Damage Identification in Aging Aircraft Structures With Piezoelectric Wafer Active Sensors," *Journal of Intelligent Material Systems and Structures*, Vol. 15, No. 9–10, pg. 673–687, 2003.
- <sup>8</sup>Cuc A., Tidwell Z., Giurgiutiu, V., and Joshi S., "Non-Destructive Evaluation (Nde) Of Space Application Panels Using Piezoelectric Wafer Active Sensors," *Proceedings of IMECE2005*, 5-11 Nov., paper# IMECE2005-81721
- <sup>9</sup>Kessler S. S., Spearing M. S., Soutis C., "Damage detection in composite materials using Lamb wave methods", *Smart Materials and Structures*, August, 2001
- <sup>10</sup>Saravanos D. A., Birman V., Hopkins D. A., "Detection of delaminations in composite beams using piezoelectric sensors", *Proceedings of the 35<sup>th</sup> Structures, Structural Dynamics and Materials Conference (AIAA)*, 1994.
- <sup>11</sup>Keilers C. H., Chang F. K., "Identifying delamination in composite beams using built-in piezocersamics: Part I – experiments and analysis", *Journal of Intelligent Material Systems and Structures*, Vol. 6, 1995
- <sup>12</sup>Zhongqing S., Ye, L., "Lamb wave propagation-based damage identification for quasi-isotropic CF/EP composite laminates using artificial neural algorithm: Part II - Implementation and validation" *Journal of Intelligent Material Systems and Structures*, Vol. 16, 2005.
- <sup>13</sup>Matt H., Bartoli I., Lanza di Scalea F., "Ultrasonic guided wave monitoring of composite wing skin-to-spar bonded joints in aerospace structures" *Journal of Intelligent Materials*, 2005.
- <sup>14</sup>Giurgiutiu, V., "Tuned Lamb-Wave Excitation and Detection with Piezoelectric Wafer Active Sensors for Structural Health Monitoring", *Journal of Intelligent Material Systems and Structures*, Vol. 16, No. 4, pp. 291-306, 2005
- <sup>15</sup>Raghavan A., Cesnik C. E. S., "Modeling of piezoelectric-based Lamb-wave generation and sensing for structural health monitoring"; *Smart Structures and Materials*, 2004, pp. 419-430.
- <sup>16</sup>Bottai G. S., Giurgiutiu V., "Lamb wave interaction between piezoelectric wafer active sensors and host structure in a composite material", *5<sup>th</sup> IWSHM5 Stanford University*, 2005